Meteoritics & Planetary Science 42, Nr 1, 49–61 (2007)
Abstract available online at http://meteoritics.org

Hydrothermal alteration experiments of enstatite: Implications for aqueous alteration of carbonaceous chondrites

Ichiro OHNISHI[1*] and Kazushige TOMEOKA[1, 2]

[1]Graduate School of Science and Technology, Kobe University, Kobe 657-8501, Japan
[2]Department of Earth and Planetary Sciences, Faculty of Science, Kobe University, Kobe 657-8501, Japan
[*]Corresponding author. E-mail: ichiro@kobe-u.ac.jp

(Received 28 March 2006; revision accepted 04 November 2006)

Abstract–Enstatite is one of the major constituent minerals in carbonaceous chondrites. Hydrothermal alteration experiments (26 in total) of enstatite were carried out at pH 0, 6, 7, 12, 13, and 14, at temperatures of 100, 200, and 300 °C, and for run durations of 24, 72, 168, and 336 h in order to provide constraints on the aqueous-alteration conditions of the meteorites. The recovered samples were studied in detail by using powder X-ray diffraction, scanning electron microscopy (SEM), and transmission electron microscopy (TEM).

Under acidic and mildly acidic conditions (pH 0, 6), no significant alteration occurred, whereas under neutral to alkaline conditions (pH 7–14), serpentine and saponite formed in various proportions by replacing enstatite. At 300 °C for 168 h, serpentine formed under neutral to moderately alkaline conditions (pH 7, 12), and serpentine and saponite formed as unit cell-scale coherent intergrowths under highly alkaline conditions (pH 13, 14). The amounts of phyllosilicates have a tendency to increase with increasing pH, temperature, and run duration. There is also a tendency for saponite to form at higher pH and temperature and under longer run-durations than serpentine.

The results indicate that alteration of enstatite is strongly dependent on the experimental conditions, especially pH. They suggest that CM chondrites experienced aqueous alteration under neutral to alkaline conditions, whereas CV and CI chondrites experienced aqueous alteration under more alkaline conditions. The results also suggest that aqueous alteration in CI chondrites occurred at higher temperatures than in CM chondrites, and aqueous alteration in CV chondrites occurred at even higher temperatures than in CI chondrites.

INTRODUCTION

Carbonaceous chondrites of types 1–3 (CI, CM, CR, CO, and CV) and some unequilibrated ordinary chondrites contain various amounts of hydrous minerals, mainly phyllosilicates (e.g., Barber 1981; Tomeoka and Buseck 1985, 1988, 1990; Weisberg et al. 1993; Keller and Buseck 1990a, 1990b; Brearley 1993, 1997; Hutchison et al. 1987). Major fractions of micrometeorites and interplanetary dust particles are also similar in chemistry and mineralogy to the hydrous matrices of CI and CM chondrites (e.g., Kurat et al. 1994; Sandford and Bradley 1989). Most of the hydrous minerals are regarded to have formed by reactions of primary anhydrous minerals with aqueous fluids on their parent bodies. Thus, the widespread occurrence of hydrous minerals in those primitive materials suggests that aqueous alteration was a major physical and chemical process that occurred widely in the early solar system.

Previous mineralogical and petrological studies have shown that hydrous minerals differ among the different types of chondrite (Table 1 and references therein). For example, the matrices of CI chondrites consist mainly of serpentine, saponite, and ferrihydrite, the matrices of CM chondrites consist mainly of serpentine and tochilinite, and the matrices of hydrated CV chondrites contain saponite. Mineralogical and petrological studies (e.g., Tomeoka and Buseck 1988, 1990; Keller and Buseck 1990b; Keller et al. 1994; Zolensky et al. 1989, 1993; Zega et al. 2003; Jones and Brearley 2006) and oxygen isotopic studies (e.g., Clayton and Mayeda 1999) suggest that the differences in hydrous minerals may have resulted from differences in alteration conditions, such as temperature, pH, compositions of aqueous fluids, oxygen fugacity, and water/rock ratio, on the meteorite parent bodies.

Experimental research can provide insight into the conditions under which carbonaceous chondrites were altered. In the past, a few workers have conducted

Table 1. Major hydrous phases in the carbonaceous chondrites.

Meteorite	Hydrous phase	Composition	References
CI	Serpentine	$(Mg, Fe)_3Si_2O_5(OH)_4$	1, 2
	Saponite	$(Na, K)_{0.3}(Mg, Fe)_3(Si, Al)_4O_{10}(OH)_2 \cdot nH_2O$	
	Ferrihydrite	$5Fe_2O_3 \cdot 9H_2O$	
CM	Serpentine	$(Mg, Fe)_3Si_2O_5(OH)_4$	3–8
	Cronstedtite	$(Fe^{3+}, Fe^{2+}, Mg)_3(Fe^{3+}, Si)_2O_5(OH)_4$	
	Tochilinite	$6Fe_{0.9}S \cdot 5(Mg, Fe)(OH)_2$	
CR	Serpentine	$(Mg, Fe)_3Si_2O_5(OH)_4$	9
	Chlorite	$(Mg, Fe)_5Al(Si, Al)_4O_{10}(OH)_8$	
CV	Saponite	$(Na, K)_{0.3}(Mg, Fe)_3(Si, Al)_4O_{10}(OH)_2 \cdot nH_2O$	10–14
	Na-phlogopite	$(Na, K)(Mg, Fe)_3Si_3AlO_{10}(OH)_2$	
CO	Serpentine	$(Mg, Fe)_3Si_2O_5(OH)_4$	15, 16

References: (1) Tomeoka and Buseck (1988); (2) Brearley (1992); (3) Akai (1980); (4) Barber (1981); (5) MacKinnon and Zolensky (1984); (6) Tomeoka and Buseck (1985); (7) Zega et al. (2003); (8) Zega et al. (2004); (9) Weisberg et al. (1993); (10) Hashimoto and Grossman (1987); (11) Tomeoka and Buseck (1990); (12) Keller and Buseck (1990b); (13) Keller et al. (1994); (14) Lee et al. (1996); (15) Keller and Buseck (1990a); (16) Brearley (1993).

hydrothermal alteration experiments aimed at understanding the alteration conditions. Tomeoka and Kojima (1995) performed alteration experiments of the Allende CV chondrite with 1N-HCl solutions at 450 °C and showed that the mineralogy produced in altered Allende closely resembles that of hydrated CV chondrites such as Mokoia and Kaba. Jones and Brearley (2006) performed alteration experiments of Allende with H_2O at 100–200 °C and showed that the degree of alteration differs with temperature, run duration, and water/rock ratio. Iishi and Han (2000) showed that the proportions of serpentine and saponite produced differ with varying Fe content of olivine and temperature. Nomura and Miyamoto (1998) showed that nepheline hydrate forms from melilite under highly alkaline conditions. Despite these studies, many of the details of alteration conditions still remain unknown.

In the present study, we undertook hydrothermal alteration experiments of enstatite. Enstatite is one of the major constituents in chondrites and occurs mainly as coarse-grained phenocrysts in chondrules. Previous studies showed that enstatite has been more preferentially replaced by phyllosilicates than olivine and other major anhydrous silicates in CV and CM chondrites (e.g., Keller and Buseck 1990b; Hanowski and Brearley 2001), indicating that enstatite is very susceptible to aqueous alteration. Especially interesting is that the phyllosilicates produced from enstatite differ among the different types of chondrite. For example, saponite forms in CV chondrites (e.g., Keller and Buseck 1990b), whereas serpentine forms in CM chondrites (e.g., Hanowski and Brearley 2001). Thus, enstatite could serve as a sensitive indicator of aqueous-alteration conditions in the chondrites. However, the alteration behavior of enstatite is very poorly understood. Although there are several previous hydrothermal experimental works related to alteration of enstatite (e.g., Hemley et al. 1977; Janecky and Seyfried 1986), they mostly focused on the complex natural systems on the Earth that do not simply involve enstatite. The major goals of our study were to examine alteration products of enstatite formed under various pH, temperature, and run-duration conditions, to compare the alteration products with those in the aqueously altered carbonaceous chondrites, and to provide constraints on aqueous-alteration conditions of those chondrites.

EXPERIMENTAL

Starting Material

Orthoenstatite (OEN) single crystals (0.3–2 mm in size) were synthesized by the flux method using Li_2O-MoO_3-V_2O_5 flux (Ozima 1982). The synthesized single crystals were identified to be nearly pure Mg-endmember OEN by powder X-ray diffraction (XRD) and quantitative wavelength-dispersive X-ray spectroscopy using an electron microprobe analyzer (Table 2). As a starting material, OEN powder was prepared by grinding the synthesized OEN single crystals with an agate mortar; powder was used rather than single crystals in order to accelerate the reaction rates. Scanning electron microscope observations show that the OEN powder consists of angular to tabular grains 30–100 μm in size.

Enstatite has two polymorphs, OEN and clinoenstatite (CEN). Enstatite in most chondrites occurs as intergrowths of OEN and CEN (e.g., Brearley and Jones 1998). In the present experiments, OEN was used as a starting material because OEN is much more easily synthesized than CEN. Previous petrological studies suggest that OEN is more resistant to aqueous alteration than CEN, but their alteration products are similar to each other (e.g., Hanowski and Brearley 2001).

Hydrothermal Alteration Experiments

Hydrothermal alteration experiments of enstatite were carried out at temperatures of 100, 200, and 300 °C, and for

Table 2. Compositions of OEN before reaction and alteration products of the runs with various solutions at 300 °C for 168 h (wt%).

	OEN		Alteration product									
			1N-HCl		H_2O		0.01N-NaOH		0.1N-NaOH		1N-NaOH	
Initial pH			0		7		12		13		14	
Number of analyses	50	(s.d.)	13	(s.d.)	7	(s.d.)	10	(s.d.)	14	(s.d.)	17	(s.d.)
Na_2O	–	(–)	–	(–)	–	(–)	0.32	(0.13)	0.56	(0.07)	0.43	(0.07)
MgO	60.1	(0.3)	6.96	(8.12)	25.6	(0.8)	21.2	(2.4)	28.8	(2.2)	30.3	(3.6)
SiO_2	40.8	(0.3)	76.4	(8.0)	42.9	(0.9)	32.8	(4.2)	41.3	(3.1)	43.8	(4.9)
Total	101.1		83.6		68.8		54.3		70.7		74.5	
Mg/Si (atomic ratio)	1.01		0.14		0.89		0.97		1.04		1.03	

OEN was analyzed by WDS, whereas all the alteration products were analyzed by EDS.
s.d. = standard deviation.

run durations of 24, 72, 168, and 336 h (conditions are summarized in Table 3). These experimental conditions were chosen in reference to the previous hydrothermal experiments of olivine (e.g., Tomita 1969; Yada and Iishi 1974; Takatori et al. 1993; Nomura and Miyamoto 1998), which were carried out under the conditions of <100–450 °C and from 1 week to 2 months. Since olivine is the dominant anhydrous silicate in unaltered chondrites, we hypothesized that comparing the alteration behaviors of olivine and enstatite would be helpful in understanding the alteration of chondrites.

Hydrothermal experiments at 100 and 200 °C were performed with a Teflon reaction cell of 4 cm^3 loaded into a Morey-type autoclave (Table 3). In each run, 50 mg of OEN powder was reacted with a 2 cm^3 solution under the saturated steam pressure. The weight ratio of aqueous solution to OEN is constant (~40) in all the runs at 100 and 200 °C. After heating, the autoclave was cooled to room temperature in air, and solid samples were separated from residual liquids and dried in air.

Hydrothermal experiments at 300 °C were performed with a test-tube-type hydrothermal apparatus (NIKKISO HTU1-NK-H25-II) (Table 3). In each run, 30 mg of OEN powder and a 0.1 cm^3 solution were sealed in an Au capsule, loaded into a high-pressure reaction vessel in the hydrothermal apparatus, and heated at 300 °C under 1 kb. The weight ratio of aqueous solution to OEN is constant (~3.3) in all the runs at 300 °C. It should be noted that, because of the limitation of the internal volume of the reaction vessel, the solution/OEN ratio needed to be set much lower than that in the runs at 100 and 200 °C. After heating, the reaction vessel was quenched with ice water. After opening the capsule, solid samples were separated from residual liquids and dried in air.

In order to examine alteration products of enstatite over almost the entire range of pH, the following six solutions were used to react with the OEN powder: 1N-HCl (pH 0), 1N-NaCl (pH 6), H_2O (pH 7), 0.01N-NaOH (pH 12), 0.1N-NaOH (pH 13), and 1N-NaOH (pH 14) (Table 3). The pH of the solutions was measured with a pH meter (HORIBA F-12) at room temperature.

Characterization of Materials

The synthesized single crystals of OEN were examined with an X-ray diffractometer (RIGAKU RINT2000), operated at 30 kV and 12 mA with a Cu Kα radiation, and an electron microprobe analyzer (JEOL JXA-8900), equipped with wavelength-dispersive X-ray spectrometers (WDS). WDS analyses with the electron microprobe analyzer were obtained at 15 kV and 12 nA.

All the recovered samples were initially examined with an optical stereo microscope and XRD. Some of the samples were embedded in epoxy and polished sections were made. These sections were studied using a scanning electron microscope (SEM) (JEOL JSM-5800) equipped with an energy-dispersive X-ray spectrometer (EDS). EDS analyses with the SEM were obtained at 15 kV and 0.4 nA. An Oxford Link ISIS analytical system was used for the EDS analyses. Data corrections were made by the Phi-Rho-Z method. Well-characterized minerals and glasses were used as standards for quantitative analyses. For the analysis of each mineral grain, we used a focused electron beam of ~2 μm in diameter. Some of the recovered samples were embedded in epoxy and processed to thin foils of ~70 nm in thickness using an ultramicrotome. The thin foils were mounted on a Cu grid covered with a formvar/carbon film and studied using a transmission electron microscope (TEM) (JEOL JEM-2010) operated at 200 kV. Identification of crystal structure was based on selected-area electron diffraction (SAED) and high-resolution imaging.

RESULTS

Our hydrothermal alteration experiments of enstatite under various pH, temperature, and duration conditions have produced a variety of alteration products. Experimental conditions and alteration products of all the runs (26 in total) are summarized in Table 3. The XRD measurements of all the recovered samples show that they contain various amounts of unaltered OEN. Our descriptions of XRD measurements will focus on the alteration products; the

Table 3. Experimental conditions and alteration products.

Run no.	Starting material	Solution		Initial pH	Temperature (°C)	Duration (h)	Product
1	OEN	HCl	1N	0	200	72	Am-Si
2	OEN	HCl	1N	0	300	24	Am-Si
3	OEN	HCl	1N	0	300	168	Am-Si
4	OEN	HCl	1N	0	300	336	Am-Si
5	OEN	NaCl	1N	6	200	168	No change
6	OEN	NaCl	1N	6	300	168	No change
7	OEN	H_2O		7	100	168	No change
8	OEN	H_2O		7	200	168	No change
9	OEN	H_2O		7	200	336	No change
10	OEN	H_2O		7	300	24	No change
11	OEN	H_2O		7	300	72	No change
12	OEN	H_2O		7	300	168	Serp
13	OEN	H_2O		7	300	336	Serp
14	OEN	NaOH	0.01N	12	200	168	Serp
15	OEN	NaOH	0.01N	12	300	168	Serp
16	OEN	NaOH	0.1N	13	200	168	Serp
17	OEN	NaOH	0.1N	13	300	168	Serp + Sap
18	OEN	NaOH	1N	14	100	168	No change
19	OEN	NaOH	1N	14	100	336	No change
20	OEN	NaOH	1N	14	200	24	Serp
21	OEN	NaOH	1N	14	200	72	Serp
22	OEN	NaOH	1N	14	200	168	Serp + Sap
23	OEN	NaOH	1N	14	300	24	Serp + Sap
24	OEN	NaOH	1N	14	300	72	Serp + Sap
25	OEN	NaOH	1N	14	300	168	Serp + Sap
26	OEN	NaOH	1N	14	300	336	Serp + Sap

OEN = orthoenstatite; Am-Si = amorphous silica; Serp = serpentine; Sap = saponite.

diffraction peaks of OEN will not be mentioned unless otherwise noted.

The XRD patterns of the samples recovered from the six runs at 300 °C and for 168 h (Runs 3, 6, 12, 15, 17, and 25) are compared to each other and to that of untreated OEN in Fig. 1. This condition (300 °C/168 h) is the only one under which all six different solutions (pH 0, 6, 7, 12, 13, and 14) used in our experiments were reacted with OEN; thus, the comparison is especially useful to consider the effects of pH on the results of alteration. Compositions of the alteration products of those six runs obtained by SEM-EDS analysis are shown in Table 2 and also compared in terms of Mg/Si ratios in Fig. 2.

Reaction with Acidic Solutions (1N-HCl, 1N-NaCl)

1N-HCl Solutions (pH 0)

In XRD patterns from all four samples (Runs 1–4 in Table 3), no new diffraction peaks were detected except that the backgrounds at $2\theta = 20–30°$ are slightly enlarged (Fig. 1). The SEM-EDS observations reveal that OEN grains have been partially replaced by a SiO_2-rich material (Mg/Si = 0.14 on average), along their edges (Fig. 3), that shows low analytical totals (83.6 wt% on average) (Table 2; Fig. 2). The SAED patterns from the SiO_2-rich material, obtained with the TEM, exhibit no particular diffraction spots, indicating that it is amorphous. From these results, the SiO_2-rich material is probably amorphous silica. The enlarged backgrounds at $2\theta = 20–30°$ in the XRD patterns can be ascribed to this material.

1N-NaCl Solutions (pH 6)

In XRD patterns from the two samples (Runs 5 and 6 in Table 3), neither new diffraction peaks nor enlarged backgrounds were detected (Fig. 1). The SEM-EDS observations confirm that OEN grains remain unchanged, indicating no alteration occurred.

Reaction with Neutral Solutions (H_2O) (pH 7)

In XRD patterns from all three samples run at 100 or 200 °C for ≥168 h (Runs 7–9 in Table 3), no new diffraction peaks were detected. Similarly, no new diffraction peaks were observed in XRD patterns from the two samples run at 300 °C for ≤72 h (Runs 10 and 11). However, the samples run at 300 °C for longer durations (168 and 336 h) (Runs 12 and 13) exhibit new small diffraction peaks at 0.74, 0.45, and 0.36 nm (Fig. 1). These peaks are interpreted as corresponding to the 001, 020, and 002 reflections of serpentine, respectively.

The SEM-EDS observations of the samples from Runs 12 and 13 show that OEN grains have been extensively replaced by a fluffy, Si-Mg-rich material (Fig. 4a) that shows slightly lower Mg/Si ratios (0.89 on average) than OEN (1.0)

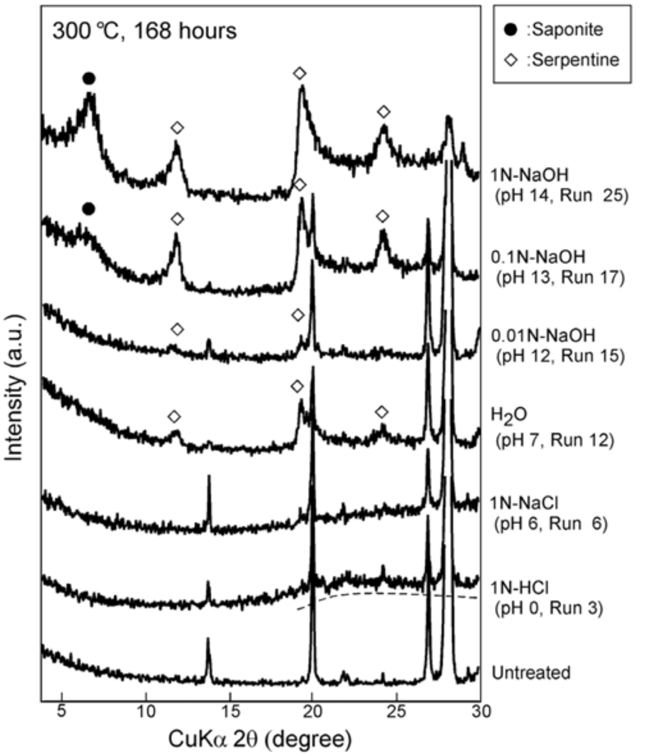

Fig. 1. Representative powder XRD patterns of untreated OEN and the samples treated at 300 °C for 168 h with 1N-HCl, 1N-NaCl, H_2O, 0.01N-NaOH, 0.1N-NaOH, and 1N-NaOH solutions (from bottom to top) (Runs 3, 6, 12, 15, 17, and 25, respectively). A slight background enlargement at $2\theta = 20$–$30°$ in the XRD pattern of the sample treated with the 1N-HCl solution is indicated by a dashed line. Indicated by filled circles are saponite peaks (1.41 nm), and indicated by open boxes are serpentine peaks (0.74, 0.45, and 0.36 nm from left to right). Other peaks are ascribed to OEN.

and very low analytical totals (68.8 wt% on average) (Table 2; Fig. 2). TEM observations of the Run 12 sample reveal that the Si-Mg-rich material contains fine fibrous crystals, which occur in packets of straight to curved layers having a layer spacing of ~0.7 nm; packets consist of several to 20 stacks of layers (Figs. 4b and 4c). We interpret these crystals as incipient serpentine. OEN crystals are replaced by serpentine along their edges and from their insides (Fig. 4b). We interpret the fluffy, Si-Mg-rich material as an intimate mixture of serpentine and a Si-Mg-rich amorphous material.

Reaction with Alkaline Solutions (0.01N-, 0.1N-, 1N-NaOH)

0.01N-NaOH Solutions (pH 12)

In XRD patterns from the two samples run at 200 and 300 °C for 168 h (Runs 14 and 15 in Table 3), small diffraction peaks of serpentine (0.74 and 0.45 nm) were detected (Fig. 1). The intensities of those peaks from the Run 15 sample are comparable to those of the sample treated with H_2O under the same condition (Run 12) (Fig. 1). The SEM-EDS observations of both Run 14 and 15 samples show that OEN grains have been partially replaced by a Si-Mg-rich material (Mg/Si = 0.97 on average) that has a composition similar to the counterpart in the sample treated with H_2O (Run 12) (Table 2; Fig. 2). This material can also be interpreted as a mixture of serpentine and a Si-Mg-rich amorphous material.

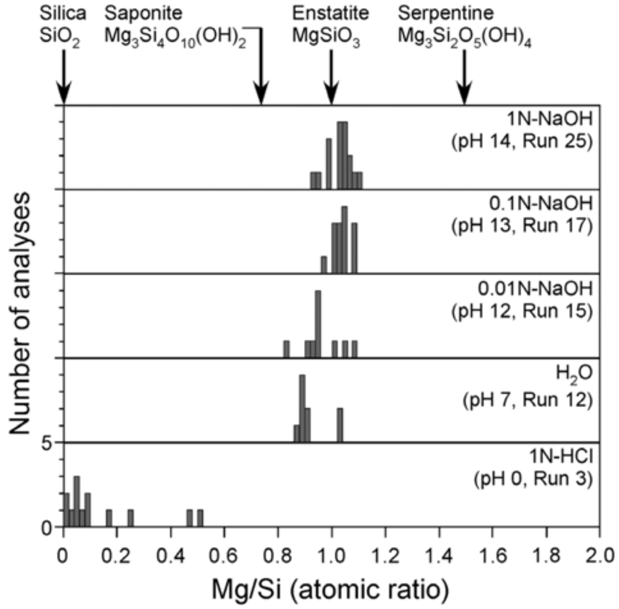

Fig. 2. A histogram of Mg/Si atomic ratios of alteration products in the samples treated at 300 °C for 168 h with 1N-HCl, H_2O, 0.01N-NaOH, 0.1N-NaOH, and 1N-NaOH solutions (from bottom to top) (Runs 3, 12, 15, 17, and 25, respectively), obtained by SEM-EDS.

0.1N-NaOH Solutions (pH 13)

Significant differences were observed in XRD patterns between the two samples run at 200 and 300 °C for 168 h (Runs 16 and 17 in Table 3). The sample run at 200 °C shows small diffraction peaks of serpentine at 0.74, 0.45, and 0.36 nm, which are comparable in intensity to those of the samples treated with H_2O and 0.01N-NaOH solution at 300 °C for 168 h (Runs 12 and 15) (Fig. 1). On the other hand, the sample run at 300 °C shows significantly larger peaks at 0.74, 0.45, and 0.36 nm, indicating that a higher abundance of serpentine was formed in the latter (Fig. 1). In addition, a new small peak was detected at 1.41 nm in the latter. After ethylene glycol treatment, the peak at 1.41 nm shifted to 1.70 nm, which can be explained by interlayer swelling. Therefore, we interpret that the peak at 1.41 nm corresponds to the 001 reflection of smectite (saponite).

The SEM-EDS observations of the sample run at 300 °C (Run 17) show that OEN grains have been extensively replaced by a Si-Mg-rich material, and most OEN grains have been nearly completely replaced, exhibiting pseudomorphic texture (Fig. 5a). The Si-Mg-rich material shows Mg/Si ratios (1.04 on average) similar to OEN and low analytical totals

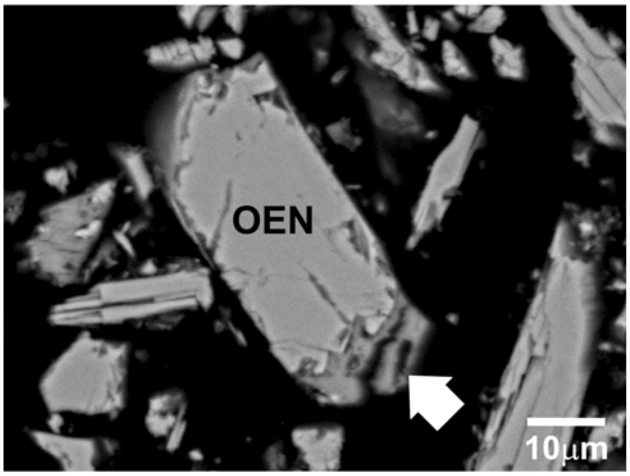

Fig. 3. A backscattered electron image of the sample treated with the 1N-HCl solution (pH 0) at 300 °C for 168 h (Run 3 in Table 3), showing that OEN grains have been partially replaced by a SiO_2-rich material (white arrow).

(70.7 wt% on average) (Table 2; Fig. 2). TEM observations reveal that the Si-Mg-rich material consists mainly of coherent intergrowths of two types of layers. One type has a relatively constant layer spacing of ~0.7 nm. The other type has a spacing of ~1.0 nm, but its layers are commonly wavy and show spacings ranging up to 1.4 nm (Figs. 5b and 5c). Both types of layers show slight curvature. We interpret the 0.7 nm and 1.0 nm layers to correspond to serpentine and saponite, respectively. The saponite layers probably collapsed incompletely to the basal spacing of 1.0 nm under the high vacuum of the TEM, thus exhibiting the variable spacings. The phyllosilicates are much more coarsely crystallized than the serpentine in the sample treated with H_2O under the same temperature and duration conditions (Run 12).

1N-NaOH Solutions (pH 14)

The samples run at 100 °C for 168 and 336 h (Runs 18 and 19 in Table 3) show no new diffraction peaks in their XRD patterns. However, the samples run at 200 °C for 24 and 72 h (Runs 20 and 21) show serpentine peaks (0.74, 0.45, and 0.36 nm), and the sample run at 200 °C for 168 h (Run 22) shows not only serpentine peaks (0.74, 0.45, and 0.36 nm), but also a saponite peak (1.41 nm). The intensities of both the serpentine and saponite peaks are comparable to those of the sample treated with the 0.1N-NaOH solution at 300 °C for 168 h (Run 17) (Fig. 1).

All four samples run at 300 °C for 24, 72, 168, and 336 h (Runs 23–26) show both the serpentine and saponite peaks in their XRD patterns (see Fig. 1 for the sample run for 168 h). The intensities of both the serpentine and saponite peaks from all four samples are larger than those in the sample run at 200 °C (Run 22). The intensities of both the serpentine and saponite peaks increase with increasing run duration from 24, 72, to 168 h, but they show no significant differences between

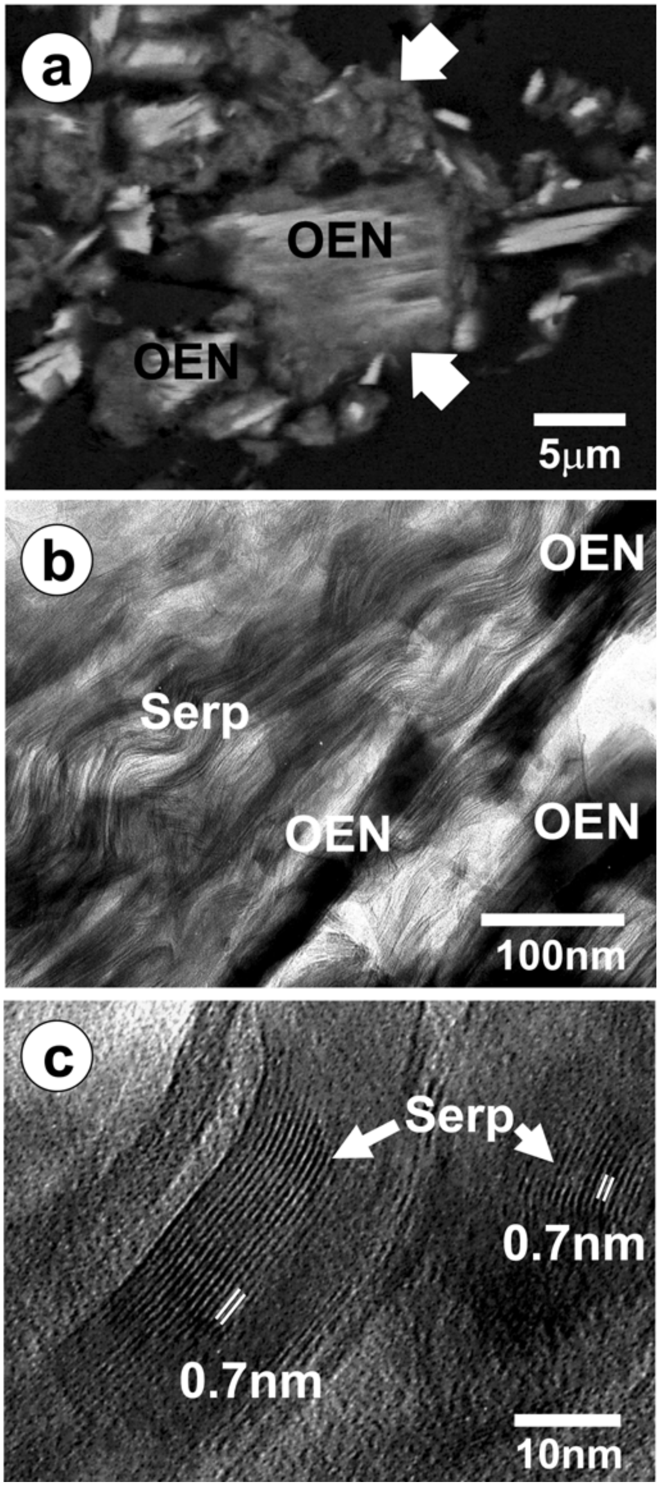

Fig. 4. a) A backscattered electron image of the sample treated with H_2O (pH 7) at 300 °C for 168 h (Run 12 in Table 3), showing that OEN grains have been extensively replaced by the Si-Mg-rich material (white arrow). b) A TEM image of the Si-Mg-rich material, showing that fibrous serpentine (Serp) crystals form by replacing OEN grains. c) A high-resolution TEM image of serpentine fibers consisting of layers with a 0.7 nm layer spacing.

the samples run for 168 and 336 h. On the other hand, the intensities of OEN peaks decrease with increasing run duration from 24 to 72 h, and they are nearly absent in the samples run for 168 h (Fig. 1) and 336 h. These observations indicate that the alteration of enstatite has nearly reached completion in the latter two samples.

The SEM-EDS observations of all four samples run at 300 °C for 24–336 h (Runs 23-26) show that OEN grains have been replaced by a Si-Mg-rich material to various degrees. In the samples run for 24 and 72 h, OEN grains have been partially replaced along a 5 to 20 μm zone from the edge, whereas in the samples run for 168 and 336 h they have been nearly completely replaced, exhibiting pseudomorphic texture. The Si-Mg-rich material has a composition similar to the counterpart in the sample treated with the 0.1N-NaOH solution at 300 °C (Table 2; Fig. 2). Although we did not perform TEM observation, we interpret the results of XRD measurements and SEM-EDS analyses as meaning that the Si-Mg-rich material consists of intergrowths of serpentine and saponite.

DISCUSSION

Alteration Products and Reaction

Effects of Solution pH

The results of our hydrothermal experiments reveal that the alteration products of enstatite differ greatly with the varying pH of the aqueous solutions. The variation of the alteration products in the runs for 168 h is shown as a function of pH of the aqueous solutions and temperature in Fig. 6. For example, in the runs at 300 °C for 168 h (Fig. 6), no crystalline phases formed at either pH 0 or 6, whereas serpentine formed at pH 7 and 12, and serpentine and saponite formed at pH 13 and 14.

We suggest that the differences in alteration products are probably related to the dissolution characteristics of enstatite. Enstatite ($MgSiO_3$) dissolves incongruently, and dissolution rates of Mg and Si differ with varying pH (e.g., Schott et al. 1981). Under acidic conditions, Mg is more preferentially released than Si, whereas under alkaline conditions, Si is more preferentially released than Mg; the former (acidic) tendency is especially strong compared with the latter (alkaline). Previous dissolution experiments of enstatite at room temperature (Schott et al. 1981; Oelkers and Schott 2001) showed that Mg and Si are released in the ratio of $Mg/Si > 2$ at pH 1, $Mg/Si \approx 1.5$ at pH 6, and $Mg/Si = 0.7–0.9$ at pH 10–12. Assuming that the dissolution behavior does not change significantly at 200–300 °C from the trend at room temperature, we presume that under acidic conditions Mg/Si ratios in solutions are too large to form any Mg-rich phyllosilicates, under neutral conditions Mg/Si ratios are favorable for the formation of serpentine ($Mg/Si = 1.5$), and under alkaline conditions Mg/Si ratios are favorable for the formation of both serpentine and saponite ($Mg/Si = 0.75$).

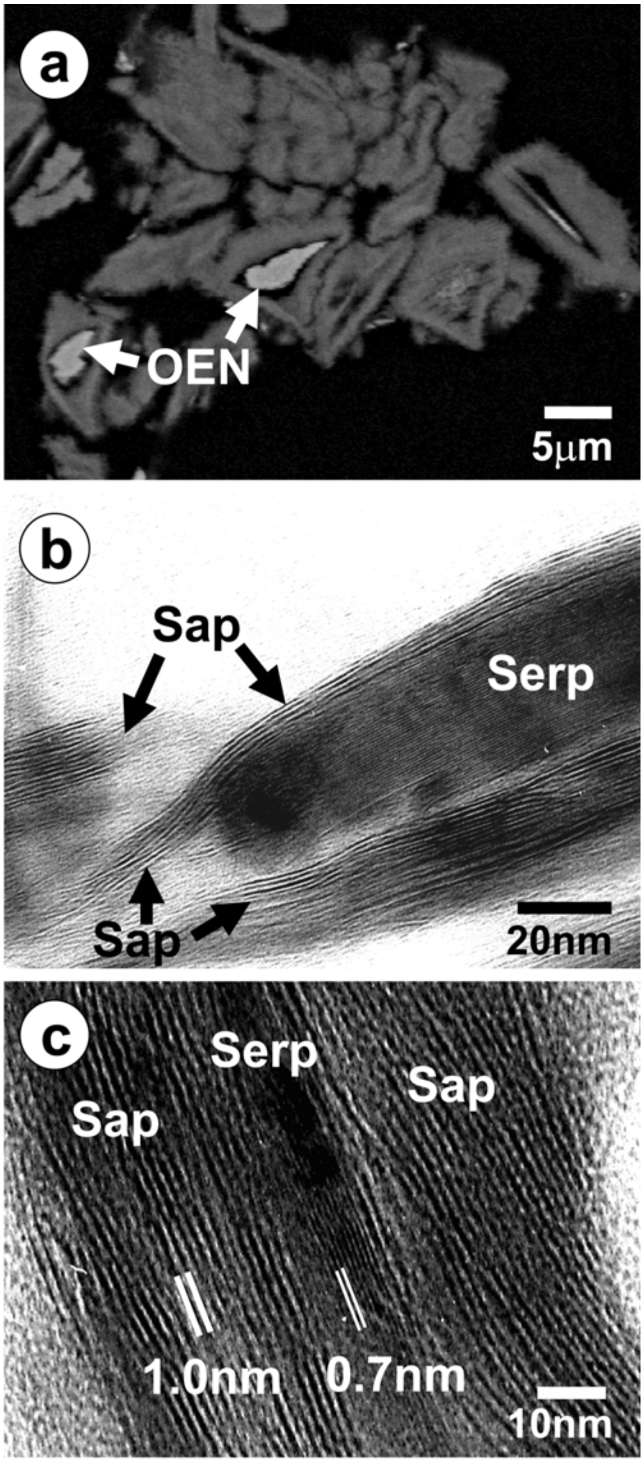

Fig. 5. a) A backscattered electron image of the sample treated with the 0.1N-NaOH solution (pH 13) at 300 °C for 168 h (Run 17 in Table 3), showing that OEN grains have been nearly completely replaced by the Si-Mg-rich material (dark gray in contrast). b) A TEM image of the Si-Mg-rich material consisting of intergrowths of serpentine (Serp) and saponite (Sap). c) A high-resolution TEM image showing that serpentine (0.7 nm layers) and saponite (1.0 nm layers) are coherently intergrown.

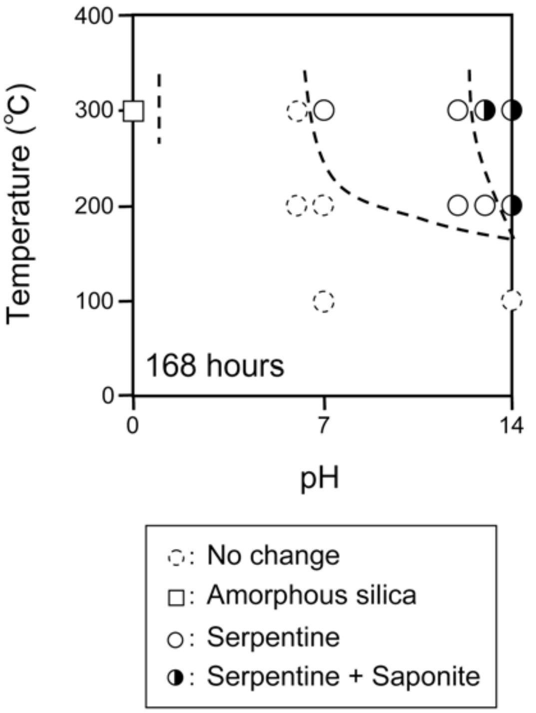

Fig. 6. The alteration products of the runs for 168 h, indicated as a function of pH of the aqueous solutions and run temperature.

Olivine is the dominant anhydrous silicate in most unaltered chondrites, and so it is worth comparing its alteration with that of enstatite. Compared with enstatite, much more hydrothermal experiments have been conducted on olivine (e.g., Tomita 1969; Yada and Iishi 1974; Takatori et al. 1993; Nomura and Miyamoto 1998). These experiments show that the alteration product of forsterite is consistently serpentine for a wide pH range (pH 3–13; data from Yada and Iishi [1974]), which differs greatly from enstatite. The difference can probably be explained by the difference in dissolution behavior between forsterite and enstatite. In contrast to enstatite, forsterite (Mg_2SiO_4) dissolves nearly congruently with the ratio of $Mg/Si \approx 2.0$ for a wide pH range (pH 1–12 at 25 °C) except for the initial stage (<1 week) of dissolution (e.g., Pokrovsky and Schott 2000). Therefore, serpentine (Mg/Si = 1.5) is regarded to be a more favorable product of alteration of forsterite than saponite (Mg/Si = 0.75).

It is significant that coherent intergrowths of serpentine and saponite formed in the aqueous alteration of enstatite under highly alkaline conditions, because such intergrowths are characteristic of the phyllosilicates in CI chondrites as discussed below. Torii et al. (1998) synthesized similar serpentine/saponite intergrowths from Si-Al-Mg hydroxide gels with Mg/(Si + Al) ratios between 0.82 and 1.1 under moderately alkaline conditions (pH 11.5-11.8 with NaOH solutions) at 300 °C. It should be noted that the Mg/(Si + Al) ratios of the starting material, the pH of the solutions and the run temperature are all very similar to those in our experiments (Mg/Si = 1, pH 13–14, and 200–300 °C). Torii et al. (1998) also found that the serpentine/saponite ratio increases from one-third to 1 to 3 with increasing Mg/(Si + Al) ratio of the starting material from 0.82, 0.93, to 1.1, respectively. These results appear to be consistent with the fact that serpentine (Mg/Si = 1.5) forms from forsterite (Mg/Si = 2.0), whereas both serpentine and saponite (Mg/Si = 0.75) form from enstatite (Mg/Si = 1.0) under highly alkaline conditions, as discussed above.

Our results also reveal that not only the mineral species but also the amounts of alteration products of enstatite differ among different pH conditions, indicating that the degree of alteration also depends on pH of aqueous solutions. For example, in the runs at 300 °C for 168 h (see Fig. 1), the amounts of serpentine that formed at pH 13 and 14 are significantly larger than those formed at pH 7 and 12, and the amount of saponite that formed at pH 14 is larger than that formed at pH 13. It is known from a great number of experimental data on syntheses of clay minerals including smectites that high pH in solutions accelerates the clay formation rate (e.g., Nagy 1995), although details of the mechanism are not well known. Those previous data are consistent with our results that the phyllosilicates form only at pH ≥ 7 and their amounts have a tendency to increase with increasing pH.

In the experiments under acidic to mildly acidic conditions (pH < 7), no alteration occurred except the formation of a minor amount of amorphous silica at pH 0 (Fig. 6). The results can be explained by high preferential dissolution of Mg from enstatite under acidic conditions as discussed above. Schott et al. (1981) also observed that amorphous silica precipitated on the surface of enstatite crystals in their dissolution experiments of enstatite at pH 1. We infer that the amorphous silica was probably produced by enhancement of Si concentrations in the vicinity of the surfaces of enstatite crystals due to preferential dissolution of Mg. Phyllosilicates are known to form when the concentration of Si in solutions is below saturation of amorphous silica (Harder 1972; Nagy 1995). Thus, the formation of amorphous silica on the surfaces of enstatite crystals (Fig. 3) probably inhibits the formation of phyllosilicates.

Effects of Temperature and Duration

The results of our hydrothermal experiments also reveal that alteration products of enstatite differ with varying temperatures and run durations. The variations of alteration products in the runs at pH 13, 14, and 7 are shown as a function of run duration and temperature in Figs. 7a, 7b, and 7c, respectively. For example, in the runs at pH 13 for 168 h (Fig. 7a), serpentine formed at 200 °C, whereas both serpentine and saponite formed at 300 °C. In the runs at pH 14 (Fig. 7b), serpentine formed at 200 °C for 24 and 72 h, whereas both serpentine and saponite formed at 200 °C for

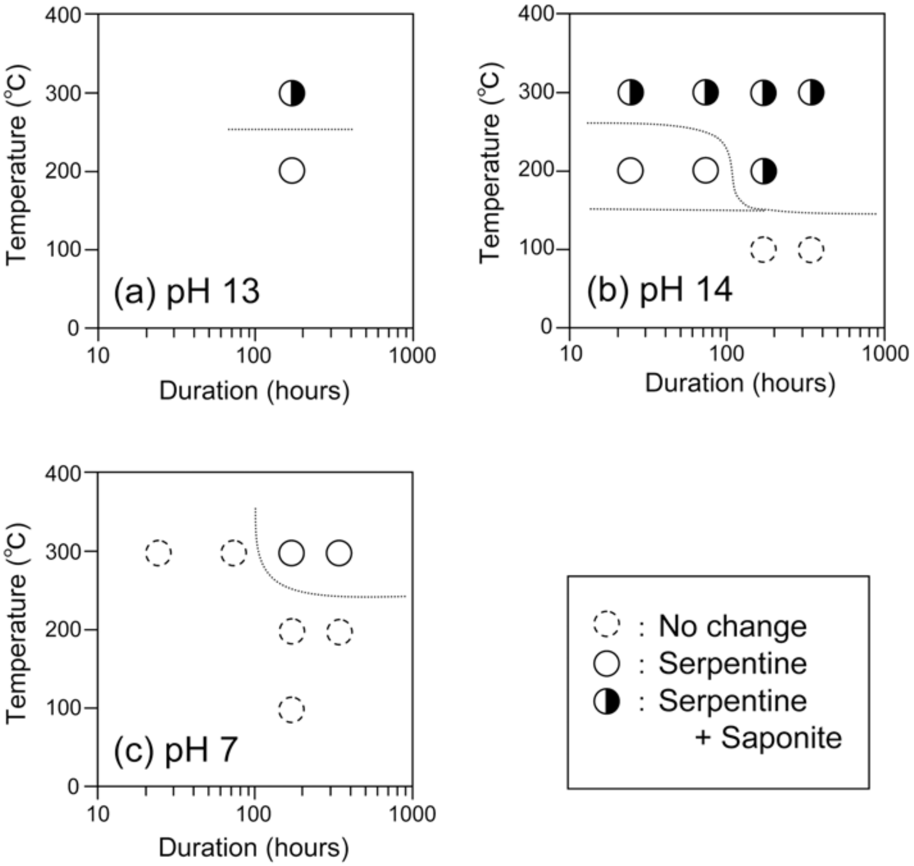

Fig. 7. The alteration products of the runs at (a) pH 13, (b) 14, and (c) 7, indicated as a function of run duration (logarithmic scale) and temperature.

168 h and at 300 °C for 24, 72, 168, and 336 h. In these runs, there is a tendency for saponite to form at a higher temperature and for a longer run-duration than serpentine. Although we are uncertain why only serpentine is formed at the lower temperature and for the shorter duration, the tendency may be explained by progressive change in composition of aqueous solutions with increasing degree of alteration. With increasing degree of serpentine (Mg/Si = 1.5) formation, Mg in solutions would preferentially be consumed, and the Mg/Si ratio in solutions progressively decreased, and as a result, became favorable for the formation of saponite (Mg/Si = 0.75).

The amounts of the phyllosilicates produced by alteration also have a general tendency to increase at higher temperatures and for longer run-durations at a given pH. For example, in the runs at pH 7 (Fig. 7c), no alteration occurred either at ≤200 °C or for ≤72 h, whereas serpentine formed at 300 °C for ≥168 h. In the runs at pH 14 (Fig. 7b), the amounts of both serpentine and saponite increase with increasing temperature and run duration. We suggest that this tendency is also related to the dissolution behavior of enstatite. The dissolution rate of enstatite is higher at a higher temperature (e.g., Oelkers and Schott 2001), and ionic concentrations in solutions increase with increasing duration of dissolution. Therefore, the degree of serpentine and saponite formation progressively increases with increasing temperature and run duration.

Mineral-Equilibrium Calculations: Comparison with the Experimental Results

In order to consider the results of our experiments in terms of mineral-equilibrium relationships, we calculated the relative stabilities of Mg-bearing species and solid phases at 0–300 °C and pH 0–14 using Geochemist's Workbench 3.2 (Bethke 1996). Figure 8 shows the calculated relative stabilities of Mg-serpentine and Mg-saponite, when Mg^{2+} and SiO_2 (aq) are dissolved species in the model solutions and both the activities are set at 10^0–10^{-2}. At any activities of Mg^{2+} and SiO_2 (aq), no solid phases are stable in the low pH field, serpentine is stable in the middle pH field, and saponite is stable in the high pH field. Although both the stability fields of serpentine and saponite change with varying activities of Mg^{2+} and SiO_2 (aq), the relative positions of the stability fields show no significant changes. These results are generally consistent with those of our hydrothermal experiments carried out at 300 °C (see Fig. 6). Therefore, we suggest that the pH

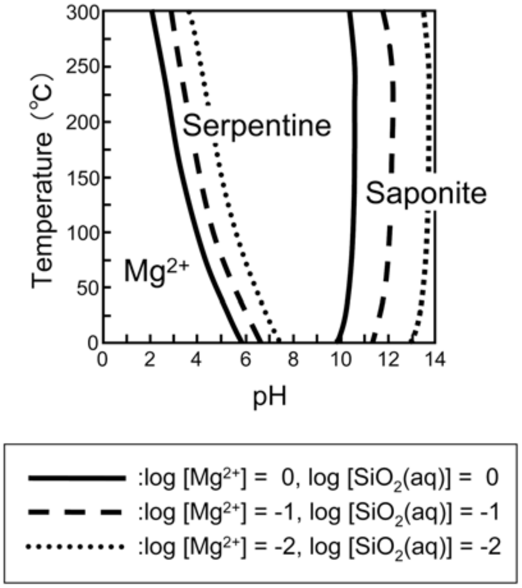

Fig. 8. The pH-temperature diagram showing the relative stabilities of Mg-bearing species and solid phases when both Mg^{2+} and SiO_2 (aq) activities are set at 10^0 (solid line), 10^{-1} (broken line), and 10^{-2} (dotted line), calculated by using Geochemist's Workbench 3.2.

dependence of alteration products of enstatite revealed by our experiments can be explained by not only the dissolution mechanism of enstatite as discussed above but also the mineral stabilities.

Implications for Aqueous Alteration in Meteorites

CV Chondrites

Most CV chondrites have been unaffected by aqueous alteration, and their matrices consist mainly of fine-grained Fe-rich olivine and a variety of minor phases such as magnetite and Fe-Ni metal/sulfide (e.g., Krot et al. 1995). Enstatite occurs mainly as coarse-grained phenocrysts in chondrules. However, some CV chondrites such as Mokoia, Kaba, and Bali have experienced minor degrees of aqueous alteration, and enstatite in those chondrites has been replaced by saponite (e.g., Tomeoka and Buseck 1990; Keller and Buseck 1990b; Keller et al. 1994). From the results of our experiments, this evidence suggests that aqueous alteration in those CV chondrites occurred under relatively high pH conditions.

Iron-rich olivine ($Fa_{\sim 50}$) in the matrices of Mokoia, Kaba, and Bali has also been partially replaced by saponite, although to lesser degrees than enstatite (Tomeoka and Buseck 1990; Keller and Buseck 1990b; Keller et al. 1994). Iishi and Han (2000) performed hydrothermal alteration experiments of Fe-rich olivine (Fa_{50}) treated with solutions with different concentrations of Na, Al, and Si at 100–200 °C. They found that serpentine forms in the solution with low concentrations of Na, Al, and Si, whereas saponite forms in the solution with high concentrations of Na, Al, and Si. From these results, they suggested that relatively alkaline and Na, Al, and Si-rich conditions are required to form saponite from Fe-rich olivine. Our interpretation that aqueous alteration in Mokoia, Kaba, and Bali occurred under relatively alkaline conditions is consistent with their results.

An alkaline condition may be indigenous to the aqueous activity on the CV parent body. Alternatively, the condition may have been realized transiently at the beginning of alteration. Previous TEM studies (e.g., Tomeoka and Buseck 1990; Keller and Buseck 1990b) showed that chondrule mesostasis in the CV chondrites is more preferentially replaced by phyllosilicates than any other constituents. The primary mesostasis consists mainly of Na-, Ca-, and Al-rich plagioclase and feldspathic glass. Dissolution experiments of plagioclase and feldspathic glass (Oelkers and Schott 1995; Hamilton et al. 2000) showed that Na and Ca ions in these minerals are preferentially released and exchanged with H^+ in solution, resulting in an increase in pH. Therefore, it is possible that, at the beginning of aqueous alteration of CV chondrites, the preferential alteration of chondrule mesostasis increased pH in the solutions and produced conditions favorable for the formation of saponite from enstatite.

The Allende CV3 chondrite also contains hydrous minerals, although in much lesser amounts than Mokoia, Kaba, and Bali, suggesting that Allende has experienced minor aqueous alteration (Tomeoka and Buseck 1982a, 1982b; Hashimoto and Grossman 1987; Keller and Buseck 1991; Brearley 1997). However, neither saponite nor serpentine has been reported from Allende. Brearley (1997) showed that talc and amphibole have been produced by alteration of enstatite in Allende chondrules. Hydrothermal alteration experiments of mixtures of enstatite and forsterite treated with H_2O at 450 °C and >1 kb (Cohen et al. 2004) showed that talc is formed by replacing enstatite. Phase-equilibrium experiments (Hemley et al. 1977) and calculations (Berman 1988) in the system MgO-SiO_2-H_2O indicated that talc can be stable at temperatures >400 °C and pressures ~1 kb. These results suggest that aqueous alteration in Allende occurred at a higher temperature than the other CV chondrites.

CM Chondrites

CM chondrites have experienced much more extensive aqueous alteration than CV chondrites, and their matrices consist mainly of Mg-Fe serpentines and tochilinite (Barber 1981; Tomeoka and Buseck 1985; Zolensky et al. 1993; Zega et al. 2003, 2004). Smectite is extremely rare in CM chondrites except for Bells (Brearley 1995). Enstatite occurs primarily as phenocrysts in chondrules and has been replaced by Mg-Fe serpentine to various degrees (e.g., Hanowski and Brearley 2001). From the results of our experiments, the evidence suggests that aqueous alteration in CM chondrites occurred under neutral to moderately alkaline conditions and at lower temperatures relative to CV chondrites.

Oxygen isotope measurements (Clayton and Mayeda

1984, 1999) suggested that aqueous alteration in CM chondrites occurred at relatively low temperatures (0–20 °C). Computer code simulations of aqueous alteration on the CM parent body (Zolensky et al. 1989; Rosenberg et al. 2001) suggested that the aqueous alteration occurred at relatively low temperatures (1–25 °C) and the pH in the aqueous solutions changed progressively from 7 to 12 with increasing degree of alteration. Hydrothermal experiments (Kakos et al. 1994; Kozerenko et al. 1996) showed that tochilinite can be produced from Fe sulfide/hydroxide at pH 7.8–11.5. Our interpretation that aqueous alteration in CM chondrites occurred under neutral to moderately alkaline conditions and at lower temperatures relative to CV and CI chondrites (see below) is consistent with these interpretations and results.

However, it should be noted that the aqueous alteration in CM chondrites may be related to not only pH/temperature but also other parameters such as oxygen fugacity and precursor mineralogy. For example, tochilinite is known to form under low oxygen fugacity (Kakos et al. 1994; Kozerenko et al. 1996), suggesting that aqueous alteration in CM chondrites occurred under reducing conditions. In CM chondrites, not only enstatite but also a variety of Mg-Fe-rich minerals such as Mg-Fe olivine, Fe-Ni metal, and Fe sulfide have been involved in extensive aqueous alteration (e.g., Tomeoka and Buseck 1985; Hanowski and Brearley 2001). It is possible that aqueous alteration of such Mg-Fe-rich minerals increased the (Mg + Fe)/Si ratio of aqueous solutions, thus promoting the formation of serpentine rather than saponite as discussed in the Effects of Solution pH section.

CI Chondrites

CI chondrites consist almost entirely of fine-grained matrix that is mainly composed of serpentine, saponite, and ferrihydrite (Tomeoka and Buseck 1988; Brearley 1992) and contain little amounts of anhydrous silicates. The mineralogy is regarded to have resulted from even more extensive aqueous alteration than in CM chondrites (e.g., Zolensky et al. 1989). Thus, it is difficult to deduce the precursors of the phyllosilicates. Serpentine and saponite in CI chondrites occur as characteristic unit cell-scale coherent intergrowths (Tomeoka and Buseck 1988; Brearley 1992). Our results indicate that such intergrowths can be produced by alteration of enstatite. The hydrothermal experiments done by Torii et al. (1998) also showed that such intergrowths can be produced from Si-Al-Mg hydroxide gels with Mg/(Si + Al) ratios close to that of enstatite (=1). These results suggest that the phyllosilicates in CI chondrites may have been formed from a material having a (Mg + Fe)/(Si + Al) ratio close to that of enstatite (= 1).

In the alteration experiments of Allende with H_2O at 100–200 °C, Jones and Brearley (2006) found that serpentine/saponite intergrowths are formed by replacing Fe-rich olivine. However, as mentioned above, in the alteration experiments of olivine (forsterite), the primary product is serpentine and no such intergrowths were reported (e.g., Tomita 1969; Yada and Iishi 1974; Takatori et al. 1993; Nomura and Miyamoto 1998). The Allende-matrix sample that Jones and Brearley (2006) studied is a complex mineral assemblage containing not only olivine but also a variety of other minerals. Thus, it is difficult to evaluate the alteration effects of a single mineral. In this regard, it is noteworthy that previous TEM observations (Tomeoka and Buseck 1990; Keller et al. 1994) revealed evidence that Fe-rich olivine in the matrices of Mokoia and Bali CV3 chondrites precipitated Fe oxide or hydroxide before or during hydration to form saponite. The CI chondrites appear to have been altered under relatively oxidizing conditions (e.g., Zolensky et al. 1993). From these observations and our experiments, we infer that, if the precursor of CI phyllosilicates was Fe-rich olivine, Fe would be preferentially released from olivine by oxidation, and the olivine would transform to an Fe-deficient structure (reduced in the [Mg + Fe]/Si ratio to <2) and thus become favorable to form serpentine/saponite intergrowths.

Our results show that the serpentine/saponite intergrowths formed from enstatite at high pH (13–14) and higher temperatures than only serpentine (Figs. 7a and 7b), suggesting that aqueous alteration in CI chondrites occurred at higher pH and temperatures relative to CM chondrites. The computer code simulations done by Zolensky et al. (1989) suggested that aqueous alteration in CI chondrites occurred at temperatures of 50–150 °C, which are higher than those for CM chondrites (1–25 °C). Based on oxygen isotope measurements, Clayton and Mayeda (1999) suggested that aqueous alteration in CI chondrites occurred at higher temperatures (~150 °C) than that in CM chondrites (0–20 °C). Our data are consistent with all these interpretations. Our results also show that the proportion of serpentine and saponite has a tendency to decrease with increasing temperature. Thus, CI chondrites likely experienced aqueous alteration at lower temperatures than CV chondrites.

CONCLUSIONS

Our experimental study has revealed that aqueous alteration of enstatite strongly depends on pH of the aqueous solutions and to lesser degrees on temperature and run duration. Under acidic conditions ($pH \leq 6$), no significant alteration occurred at any temperatures (100–300 °C) for any run durations (24–336 h). In comparison, under neutral to alkaline conditions (pH 7–14), serpentine and saponite formed in various proportions by replacing enstatite. The amount of phyllosilicates has a tendency to increase with increasing pH, temperature, and run duration. The proportion of serpentine and saponite has a tendency to decrease with increasing pH, temperature, and run duration. The differences in alteration can be mainly explained by the dissolution characteristics of enstatite.

The results indicate that the phyllosilicate mineralogy produced by alteration of enstatite in the chondrites can serve as a sensitive indicator of aqueous-alteration conditions on their parent bodies. The results suggest that the differences in phyllosilicate mineralogy among the different types of chondrite mainly resulted from different pH conditions of aqueous solutions. Aqueous alteration of CM chondrites probably occurred under neutral to alkaline conditions, whereas aqueous alteration of CV and CI chondrites occurred under more alkaline conditions. The results also suggest that CI chondrites experienced alteration at higher temperatures than CM chondrites, and CV chondrites experienced alteration at higher temperatures than CI chondrites.

Acknowledgments–We thank Dr. S. Tachibana for assistance with sample preparations and Profs. K. Tomita and N. Sakamoto for helpful suggestions for hydrothermal alteration experiments. We also thank Dr. T. Uchino for assistance with powder X-ray diffraction, Drs. N. Tomioka, K. Nakamura-Messenger, and T. Kojima for assistance with transmission electron microscopy and useful discussions. Helpful reviews by Drs. T. Zega, L. Chizmadia, and A. Brearley are gratefully acknowledged. Powder X-ray diffraction was performed at the Department of Chemistry, Kobe University, Japan. Transmission electron microscopy was performed at the Instrumentation Analysis Division in the Center for Supports to Research and Education Activities, Kobe University, Japan. This work was supported by The 21st Century COE Program of Origin and Evolution of Planetary Systems and Grant-in-Aid (no. 16204042) of the Ministry of Education, Science, Culture, Sports, and Technology.

Editorial Handling—Dr. Christine Floss

REFERENCES

Akai J. 1980. Tubular form of interstratified mineral consisting of a serpentine-like layer plus two brucite-like sheets newly found in the Murchison (C2) meteorite. *Proceedings of the Fifth Symposium on Antarctic Meteorites*. pp. 299–310.

Barber D. J. 1981. Matrix phyllosilicates and associated minerals in C2M carbonaceous chondrites. *Geochimica et Cosmochimica Acta* 45:945–970.

Berman R. G. 1988. Internally-consistent thermodynamic data for minerals in the system Na_2O-K_2O-CaO-MgO-FeO-Fe_2O_3-Al_2O_3-SiO_2-TiO_2-H_2O-CO_2. *Journal of Petrology* 29:445–522.

Bethke C. M. 1996. *Geochemical reaction modeling: Concepts and applications*. New York: Oxford University Press. 397 p.

Brearley A. J. 1992. Mineralogy of fine-grained matrix in the Ivuna CI carbonaceous chondrite (abstract). 23rd Lunar and Planetary Science Conference. p. 153.

Brearley A. J. 1993. Matrix and fine-grained rims in the unequilibrated CO3 chondrite, ALHA77307: Origins and evidence for diverse, primitive nebular dust components. *Geochimica et Cosmochimica Acta* 57:1521–1550.

Brearley A. J. 1995. Aqueous alteration and brecciation in Bells, an unusual, saponite-bearing, CM chondrite. *Geochimica et Cosmochimica Acta* 59:2291–2317.

Brearley A. J. 1997. Disordered biopyriboles, amphibole, and talc in the Allende meteorite: Products of nebular or parent body aqueous alteration? *Science* 276:1103–1105.

Brearley A. J. and Jones R. H. 1998. Chondritic meteorites. In *Planetary materials*, edited by Papike J. J. Washington, D.C.: Mineralogical Society of America. 398 p.

Clayton R. N. and Mayeda T. K. 1984. The oxygen isotope record in Murchison and other carbonaceous chondrites. *Earth and Planetary Science Letters* 67:157–161.

Clayton R. N. and Mayeda T. K. 1999. Oxygen isotope studies of carbonaceous chondrites. *Geochimica et Cosmochimica Acta* 63: 2089–2104.

Cohen B. A., Brearley A. J., Ganguly J., Liermann H.-P., and Keil K. 2004. Experimental study of serpentinization reactions (abstract #1423). 35th Lunar and Planetary Science Conference. CD-ROM.

Hamilton J. P., Pantano C. G., and Brantley S. L. 2000. Dissolution of albite glass and crystal. *Geochimica et Cosmochimica Acta* 64: 2603–2615.

Hanowski N. P. and Brearley A. J. 2001. Aqueous alteration of chondrules in the CM carbonaceous chondrite, Allan Hills 81002: Implications for parent body alteration. *Geochimica et Cosmochimica Acta* 65:495–518.

Harder H. 1972. The role of magnesium in the formation of smectite minerals. *Chemical Geology* 10:31–39.

Hashimoto A. and Grossman L. 1987. Alteration of Al-rich inclusions inside amoeboid olivine aggregates in the Allende meteorite. *Geochimica et Cosmochimica Acta* 51:1685–1704.

Hemley J. J., Montoya J. W., Shaw D. R., and Luce R. W. 1977. Mineral equilibria in the MgO-SiO_2-H_2O system: II. Talc-antigorite-forsterite-anthophyllite-enstatite stability relations and some geologic implications in the system. *American Journal of Science* 277:353–383.

Hutchison R., Alexander C. M. O'D., and Barber D. J. 1987. The Semarkona meteorite: First recorded occurrence of smectite in an ordinary chondrite, and its implications. *Geochimica et Cosmochimica Acta* 51:1875–1882.

Iishi K. and Han X. J. 2000. Iron-rich olivine altered experimentally in alkaline solution: A study on aqueous alteration of Bali CV3 and Lance CO3 chondrites. *Neues Jahrbuch für Mineralogie—Monatshefte* 2:49–59.

Janecky D. R. and Seyfried W. E., Jr. 1986. Hydrothermal serpentinization of peridotite within the oceanic crust: Experimental investigations of mineralogy and major element chemistry. *Geochimica et Cosmochimica Acta* 50:1357–1378.

Jones C. L. and Brearley A. J. 2006. Experimental aqueous alteration of the Allende meteorite under oxidizing conditions: Constraints on asteroidal alteration. *Geochimica et Cosmochimica Acta* 70: 1040–1058.

Kakos G. A., Turney T. W., and Williams T. B. 1994. Synthesis and structure of tochilinite: A layered metal hydroxide/sulfide composite. *Journal of Solid State Chemistry* 108:102–111.

Keller L. P. and Buseck P. R. 1990a. Matrix mineralogy of the Lancé CO3 carbonaceous chondrite: A transmission electron microscope study. *Geochimica et Cosmochimica Acta* 54:1155–1163.

Keller L. P. and Buseck P. R. 1990b. Aqueous alteration in the Kaba CV3 carbonaceous chondrite. *Geochimica et Cosmochimica Acta* 54:2113–2120.

Keller L. P. and Buseck P. R. 1991. Calcic micas in the Allende meteorite: Evidence for hydration reactions in the early solar nebula. *Science* 252:946–949.

Keller L. P., Thomas K. L., Clayton R. N., Mayeda T. K., DeHart J. M., and McKay D. S. 1994. Aqueous alteration of the Bali CV3 chondrite: Evidence from mineralogy, mineral chemistry, and oxygen isotopic compositions. *Geochimica et Cosmochimica Acta* 58:5589–5598.

Kozerenko S. V., Organova N. J., Fadeev V. V., Magazina L. O., Kolpakova N. N., and Kopneva L. A. 1996. Tochilinite produced in laboratory (abstract). 27th Lunar and Planetary Science Conference. pp. 695–696.

Krot A. N., Scott E. R. D., and Zolensky M. E. 1995. Mineralogical and chemical modification of components in CV3 chondrites: Nebular or asteroidal processing? *Meteoritics* 30:748–775.

Kurat G., Koeberl C., Presper T., Brandstätter F., and Maurette M. 1994. Petrology and geochemistry of Antarctic micrometeorites. *Geochimica et Cosmochimica Acta* 58:3879–3904.

Lee M. R., Hutchison R., and Graham A. L. 1996. Aqueous alteration in the matrix of the Vigarano (CV3) carbonaceous chondrite. *Meteoritics & Planetary Science* 31:477–483.

MacKinnon I. D. R. and Zolensky M. E. 1984. Proposed structures for poorly characterized phases in C2M carbonaceous chondrite meteorites. *Nature* 309:240–242.

Nagy K. L. 1995. Dissolution and precipitation kinetics of sheet silicates. In *Chemical weathering rates of silicate minerals*, edited by White A. F. and Brantley S. L. Washington, D.C.: Mineralogical Society of America. pp. 173–233.

Nomura K. and Miyamoto M. 1998. Hydrothermal experiments on alteration of Ca-Al-rich inclusions (CAIs) in carbonaceous chondrites: Implication for aqueous alteration in parent asteroids. *Geochimica et Cosmochimica Acta* 62:3575–3588.

Oelkers E. H. and Schott J. 1995. Experimental study of anorthite dissolution and the relative mechanism of feldspar hydrolysis. *Geochimica et Cosmochimica Acta* 59:5039–5053.

Oelkers E. H. and Schott J. 2001. An experimental study of enstatite dissolution rates as a function of pH, temperature, and aqueous Mg and Si concentration, and the mechanism of pyroxene/pyroxenoid dissolution. *Geochimica et Cosmochimica Acta* 65: 1219–1231.

Ozima M. 1982. Growth of orthoenstatite crystals by the flux method. *The Journal of the Japanese Association of Mineralogists, Petrologists and Economic Geologists* 3:97–103. In Japanese.

Pokrovsky O. S. and Schott J. 2000. Kinetics and mechanism of forsterite dissolution at 25 °C and pH from 1 to 12. *Geochimica et Cosmochimica Acta* 64:3313–3325.

Rosenberg N. D., Browning L., and Bourcier W. L. 2001. Modeling aqueous alteration of CM carbonaceous chondrites. *Meteoritics & Planetary Science* 36:239–244.

Sandford S. A. and Bradley J. P. 1989. Interplanetary dust particles collected in the stratosphere: Observations of atmospheric heating and constraints on their interrelationships and sources. *Icarus* 82:146–166.

Schott J., Berner R. A., and Sjöberg E. L. 1981. Mechanism of pyroxene and amphibole weathering—I. Experimental studies of iron-free minerals. *Geochimica et Cosmochimica Acta* 45:2123–2135.

Takatori K., Tomeoka K., Tsukimura K., and Takeda H. 1993. Hydrothermal alteration experiments of olivine with varying Fe contents: An attempt to simulate aqueous alteration of the carbonaceous chondrites (abstract). 24th Lunar and Planetary Science Conference. pp. 1389–1390.

Tomeoka K. and Buseck P. R. 1982a. Intergrown mica and montmorillonite in the Allende carbonaceous chondrite. *Nature* 299:326–327.

Tomeoka K. and Buseck P. R. 1982b. An unusual layered mineral in chondrules and aggregates of the Allende carbonaceous chondrite. *Nature* 299:327–329.

Tomeoka K. and Buseck P. R. 1985. Indicators of aqueous alteration in CM carbonaceous chondrites: Microtextures of a layered mineral containing Fe, S, O and Ni. *Geochimica et Cosmochimica Acta* 49:2149–2163.

Tomeoka K. and Buseck P. R. 1988. Matrix mineralogy of the Orgueil CI carbonaceous chondrite. *Geochimica et Cosmochimica Acta* 52:1627–1640.

Tomeoka K. and Buseck P. R. 1990. Phyllosilicates in the Mokoia CV carbonaceous chondrite: Evidence for aqueous alteration in an oxidizing environment. *Geochimica et Cosmochimica Acta* 54:1745–1754.

Tomeoka K. and Kojima T. 1995. Experimental aqueous alteration of the Allende CV3 chondrite (abstract). *Meteoritics* 30:588–589.

Tomita K. 1969. Artificial conversion of olivine into a serpentine mineral. *The Reports of the Faculty of Science, Kagoshima University* 2:27–31.

Torii K., Onodera Y., Hayashi H., Nagase T., and Iwasaki T. 1998. Hydrothermal synthesis of interstratified lizardite/saponite. *Journal of the American Ceramic Society* 81:447–449.

Weisberg M. K., Prinz M., Clayton R. N., and Mayeda T. K. 1993. The CR (Renazzo-type) carbonaceous chondrite group and its implications. *Geochimica et Cosmochimica Acta* 57:1567–1586.

Yada K. and Iishi K. 1974. Serpentine minerals hydrothermally synthesized and their microstructures. *Journal of Crystal Growth* 24/25:627–630.

Zega T. J., Garvie L. A. J., and Buseck P. R. 2003. Nanometer-scale measurements of iron oxidation states of cronstedtite from primitive meteorites. *American Mineralogist* 88:1169–1172.

Zega T. J., Garvie L. A. J., Dódony I., and Buseck P. R. 2004. Serpentine nanotubes in the Mighei CM chondrite. *Earth and Planetary Science Letters* 223:141–146.

Zolensky M. E., Bourcier W. L., and Gooding J. L. 1989. Aqueous alteration on the hydrous asteroids: Results of EQ3/6 computer simulations. *Icarus* 78:411–425.

Zolensky M., Barrett R., and Browning L. 1993. Mineralogy and composition of matrix and chondrule rims in carbonaceous chondrites. *Geochimica et Cosmochimica Acta* 57:3123–3148.